



# Effect of the morphology of films of polyaniline derivatives poly-2-[(2E)-1-methyl-2-butene-1-yl]aniline and poly-2-(cyclohex-2-en-1-yl)aniline on sensory sensitivity to humidity and ammonia vapors

R. B. Salikhov<sup>†</sup>, I. N. Mullagaliev, B. R. Badretdinov, A. D. Ostaltsova,

T. T. Sadykov, A. G. Mustafin

<sup>†</sup>salikhovrb@yandex.ru

Bashkir State University, Ufa, 450076, Russia

The influence of the morphology of polyaniline derivatives on the electrical conductivity, sensory sensitivity to air humidity of thin-film structures based on them, and the reaction to ammonia vapors has been investigated. Aniline derivatives, as well as polymers based on them, poly-2-[(2E)-1-methyl-2-butene-1-yl]aniline and poly-2-(cyclohex-2-en-1-yl), were synthesized. Using a scanning electron microscope, the morphology of the surface of thin films obtained from a solution of synthesized polymers by centrifugation on sital substrates was studied. Studying the nature of morphology is extremely important when creating sensory devices. On the basis of these polymers, samples of resistive thin-film structures were prepared, the dependence of their electrical conductivity on the relative humidity of the air and the dependence of the current passing through the sample with a change in the concentration of ammonia vapors were measured. The influence of the morphology of the surface of the films on the sensitivity of sensors to air humidity has been experimentally revealed and the prospects of using the studied films in humidity sensors have been shown. According to the experimental data, it can be seen that poly-2-[(2E)-1-methyl-2-butene-1-yl] aniline film has the highest conductivity at the same values of relative humidity.

**Keywords:** polymers, polyaniline, thin-film structures, air humidity, ammonia.

## 1. Introduction

New polymer-based materials have attracted great attention in the development of electronic sensor systems, due to their low cost, ease of manufacture, and relatively simple modulation of properties using functionalization [1]. Various materials such as organic polymers, inorganic composite materials and ceramics are widely used for sensor sensors, for example, for humidity air and various gases [2–4]. The humidity sensor is an important class of chemical sensors and is widely used in environmental monitoring, food packaging, electronics, to create human comfort, etc. [5,6]. The principle of its operation is based on changes in electrical, optical and mechanical properties at different humidity levels. As a rule, the electrical properties of the sensing element change with the adsorption of water molecules on some materials, such as polymers, metal oxides and hydrides [7]. But the main limitations of these sensitive elements are cross-sensitivity, high operating temperature, response time and not high reproducibility. There are three types of polymer-based humidity sensors: resistive, capacitive and transistor.

With the rapid development of industry, the number of polluting gases harmful to human health is increasing, and it is extremely important to detect and measure the exact amount of toxic polluting gases. Anhydrous  $\text{NH}_3$  is such a

toxic gas that causes irritation of the eyes, skin and respiratory organs [8,9].  $\text{NH}_3$ , as a polluting gas, widely exists in various spheres of human activity [10,11]. Even low concentrations of  $\text{NH}_3$  can have serious consequences for human health, such as irritation of the eyes, respiratory tract and skin, causing dizziness, nausea and fatigue [12–14]. Prolonged exposure to  $\text{NH}_3$  with a concentration of 25 ppm or more can cause respiratory diseases and even death. [15]. It is reported that the concentration of  $\text{NH}_3$  in the exhaled air of healthy people is in the range of 0.2–0.5 ppm. However, the concentration of  $\text{NH}_3$  (0.82–14.7 ppm) in patients with kidney diseases is significantly higher than in healthy people. Excess  $\text{NH}_3$  can be considered as a sign of kidney disease. [16]. Therefore, there is an urgent need to develop a gas sensor operating at room temperature capable of detecting  $\text{NH}_3$ .

The purpose of this study is to establish the effect of morphology on the sensory sensitivity of thin films of polyaniline derivatives to air humidity and ammonia vapors in the air. The most difficult thing is to find the right materials for this purpose, in particular, conductive polymers are suitable for this role. Sensors based on conductive polymers have some advantages, such as short response and recovery time. Among polymers, polyaniline (PANI) has been widely studied as a gas-sensitive polymer due to its conductive properties and chemical stability [17–19]. PANI can be

synthesized using a fast and simple polymerization technique. In addition, the size and morphology of PANI particles can be controlled during the synthesis process. Thus, the cost of manufacturing and servicing sensors should be quite low. In the groundbreaking work of Chani et al. [20], polyaniline sensors in the form of granules reacted to humidity, but the response time was approximately 3–4 minutes. Thus, the development of a new highly efficient relative humidity measurement system with good sensitivity, stability and fast response remains a relevant challenge.

Polyaniline is a conductive polymer with potential applications in the field of biomedical engineering. Using IR spectroscopy and electrical conductivity measurements, it was shown that oxidation in formic acid solutions is provided by samples with moderate electrical conductivity of the order of  $0.01\text{--}0.1\text{ S cm}^{-1}$  [21]. Despite numerous advantages of PANI as a sensitive material in resistive sensors, a large number of studies are being conducted to improve its sensitivity, selectivity and response time by changing the structure, copolymerization, varying the dopant and introducing various components into the conductive polymer [22–24]. This structural flexibility of the PANI allows it to regulate and control its physical and chemical characteristics. For example, the introduction of a substituent into a polymer increases solubility, which facilitates the formation of thin films for sensors and can induce additional interaction with the analyzed substances [25]. The variation of alloying additives also affects the physical and chemical characteristics of PANI and its derivatives, the electrical conductivity of conjugated polymers strongly depends on the level of alloying and the properties of the alloying impurity [26].

Polyaniline (PANI), a well-known conductive polymer, has become a potential contender for various electronic devices, due to its conductivity, stability, excellent environmental resistance, ease of processing and low cost of raw materials and synthesis [27,28]. The properties of polyaniline are largely determined by its structure. PANI is usually obtained by oxidative chemical polymerization of a monomer under the action of various oxidizing agents and inorganic or organic acid as an alloying agent [29]. However, its extremely low solubility in most organic solvents limits its use. To solve this problem, there are several approaches: doping with inorganic or organic acids [30–32], polymerization of substituted aniline derivatives [33–35], polymeranalogical transformations [36] and polymerization of aniline with corresponding substituted anilines [37]. The scientific literature describes various derivatives of polyaniline, the physical and chemical properties of which differ from the original. It should be noted that the production of PANI derivatives with these characteristics is likely only with careful selection of suitable monomers, oxidants, alloying agents and synthesis conditions. In particular, the morphology of the surface of this polymer, which is closely related to its electrical conductivity, is controlled by the synthesis, processing of the polymer, as well as the concentration and nature of the dopant [38,39].

It is assumed that polyaniline (PANI) has broad development prospects for  $\text{NH}_3$  sensors. Reversible doping/delegation characteristics can undergo redox reactions, which significantly improves the selectivity of the sensor for

$\text{NH}_3$ . [40]. In addition, excellent electrical conductivity and environmental resistance make PANI potential candidates for  $\text{NH}_3$  detection at room temperature. For example, in the article [41], PANI nanofibers were prepared by dilute polymerization and an  $\text{NH}_3$  sensor based on PANI was manufactured by drip casting. The sensitivity of the gas sensor based on PANI nanofibers ranges from 1.06 to 50 ppm  $\text{NH}_3$ . In [42], a quasi-two-dimensional (q2D) PANI film was synthesized at the air-water interface, and then the q2D PANI film was transferred to a  $\text{SiO}_2$  substrate coated with Au electrodes. The response of the PANI sensor is about 8%, the response time and recovery time are about 875 and 1125 s, respectively. Although  $\text{NH}_3$  gas sensors they work at room temperature, the claimed  $\text{NH}_3$  sensor based on the pure phase of PANI still has problems with low sensitivity and long response-recovery time at room temperature. Therefore, there is an urgent need to synthesize a PANI material with a higher charge transfer rate and a high response to  $\text{NH}_3$  to solve the above problems. The introduction of surfactants has proven its effectiveness in improving of electrons [43]. In addition, the growth of the material structure is controlled by the effects of diffusion and selective adsorption.

In this paper, newly synthesized polyaniline derivatives are considered, characterized by sufficiently high solubility and good film-forming properties. The solubility, particle sizes and surface morphology of thin films of new polyaniline derivatives have been studied. On the basis of thin films of these polyaniline derivatives, air humidity and ammonia vapor sensors were manufactured and their characteristics were measured.

## 2. Experimental part

For the synthesis of the monomer 2-[(2E)-1-methyl-2-butene-1-yl]aniline (Fig. 1) (M1) the following technique was used [38,39]: pre-purified with alkali and distilled 1,3-pendadiene (1) was launched into a hydrochlorination reaction using concentrated hydrochloric acid for 6 hours. The resulting product, 2-chloropentene-3 (2), was separated in a dividing funnel, dried over  $\text{MgSO}_4$ , distilled and slowly, with constant stirring, added to aniline in a ratio of 1:4. The resulting N-substituted aniline hydrochloride (3) was heated for 6 hours at  $140^\circ\text{C}$ , which resulted in the rearrangement of Kleisen with the formation of ortho- and para-isomers of the product. The ortho-product M1 was obtained by distillation under vacuum and purification from the isomer using column chromatography (petroleum ether: isopropyl alcohol, 15:1).

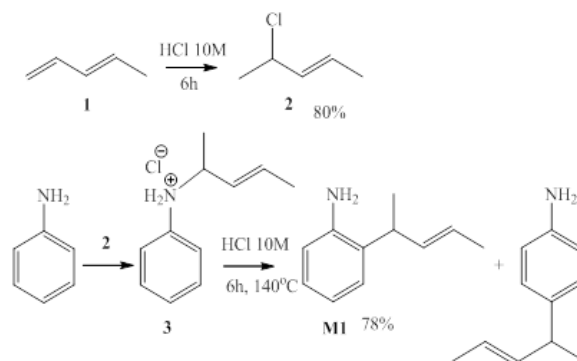


Fig. 1. Synthesis of 2-[(2E)-1-methyl-2-butene-1-yl]aniline.

The synthesis of the monomer 2-(cyclohex-2-en-1-yl)aniline (M2) (Fig. 2) was carried out according to the following procedure [46]: cyclohexanol (1) and concentrated phosphoric acid (85%) were placed in a round-bottomed flask equipped with a deflegmator, a direct refrigerator and a thermometer. The mixture is heated to a boil. Water and cyclohexene are distilled off at a temperature of 95°C. In the process of distillation, the temperature drops to 72°C. The resulting distillate is separated in a dividing funnel and dried over  $\text{CaCl}_2$ . The yield of cyclohexene is 90%. Then the resulting cyclohexene is launched into an allyl bromination reaction using N-bromosuccinimide (3). Azobisisobutyronitrile acts as a catalyst for this reaction. As a result of this reaction, 3-bromocyclohexene (4) is formed. The synthesized product was slowly, drop by drop, added to aniline in a ratio of 1: 4. The resulting N-substituted aniline hydrobromide (5) was heated at 140°C for 3–4 hours until complete rearrangement to the ortho position. The resulting M2 monomer was separated by distillation under vacuum.

Description of the synthesis of tissue polymers is presented in Fig. S1 and Fig. S2 (supplementary material).

Research methods, including the structure of the thin film resistive sensor (Fig. S3) and the setup for measuring the current-voltage characteristics of sensor samples (Fig. S4), are described in the supplementary material.

The structure of the resulting polymers was confirmed by optical spectroscopy, which is also discussed in Fig. S5 (supplementary material).

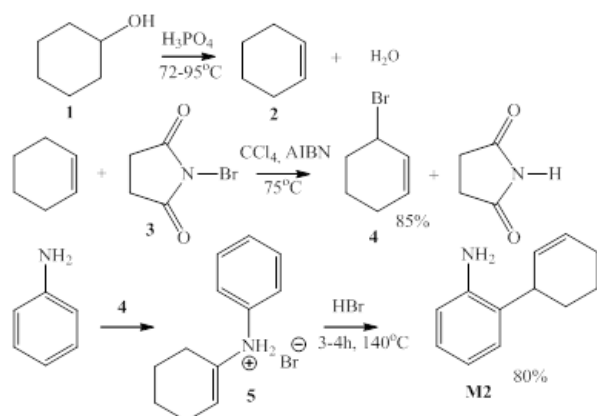


Fig. 2. Synthesis of 2-(cyclohex-2-en-1-yl)aniline.

### 3. Results and discussion

To study the effect of substituents in the polymer chain and the possibility of practical application, the solubility of P1 and P2 in organic solvents of various nature was evaluated. It is known that the main disadvantage of PANI is its low solubility in known organic solvents [26]. However, the introduction of a substituent into the aromatic ring of the polymer led to a significant increase in its solubility in dimethyl sulfoxide, N-methylpyrrolidone and chloroform. The higher solubility of polymers in organic solvents can be explained by the alkyl substituent in the polymer chain. This leads to a higher flexibility of the chain than the rigid PANI structure. Thus, the alkenyl substituent in the polymer structure has a positive effect on solubility (Table 1).

Table 1. Solubility of polymers in various solvents.

Solvent	Ability to dissolve	
	P1	P2
Chloroform	**	*
Dimethyl sulfoxide	***	***
N-methylpyrrolidone	***	***
Dimethylformamide	***	***

\* does not dissolve or does not dissolve well (<5%);

\*\* partially soluble (>10%);

\*\*\* it is well soluble (>50%)

The particle size significantly affects the value of the diffusion of gases into the polymer layer. The effect of particle size on polymerization processes is discussed in Fig. S6 (supplementary material). The results of previous studies on the use of PANI and its derivatives have shown that polymers with a porous one-dimensional morphology have the greatest sensitivity and speed, in which the efficiency does not depend on the thickness of the film [52, 53]. A polymer with this morphology is capable of forming a highly porous sensory layer with a large surface area, which increases the diffusion of gas molecules into the polymer and increases the contact area of the analyte. As a result, sensors based on such materials have high sensitivity and high performance. Based on the data on the density of the structure and large particle sizes, it can be assumed that the diffusion of gases in the films will proceed slowly, due to the difficulty of penetration of the analyte into the polymer film. While the presence of porous and smaller particles, providing a larger surface area for the analyte to contact, will contribute to a greater change in electrical conductivity with increasing humidity.

With the help of the scanning electron microscope (SEM) TESCAN MIRA LMS and the TESCAN Essence software, images of the surface of the studied polymers were obtained (Fig. 3).

The morphology of the surface of P2 is ragged, heterogeneous, with large dips in depth, which reduces the surface area available to the molecules of the analyzed gas. The surface of P1 has a homogeneous spherical globular structure, which facilitates the access of a large number of gas molecules, compared with P2.

The roughness values were obtained using the AFM image processing program Gwyddion. The RMS roughness over the Sq and surface area of the obtained films is described in Table 2.

According to the measurement results, the dependences of the current flowing through the PANI films on humidity were constructed (Fig. 4), where section 1 is the data taken with an increase in humidity in the booth chamber, and section 2 is the data with a decrease in humidity. In the figure we see the correlation of the structure of the substance and the values of currents through the films of sensory samples. P2 begins to react to humidity already at 30% due to its porous structure. The growth of current in samples with P1 begins only at 50%, it is characterized by a sharp increase in current, and the maximum value is 3 times higher than the corresponding value for samples with P2. According to the data, it can be seen that the film of the P1 sample has the highest conductivity (the conductivity is proportional to the magnitude of the current, since the applied voltage was fixed)



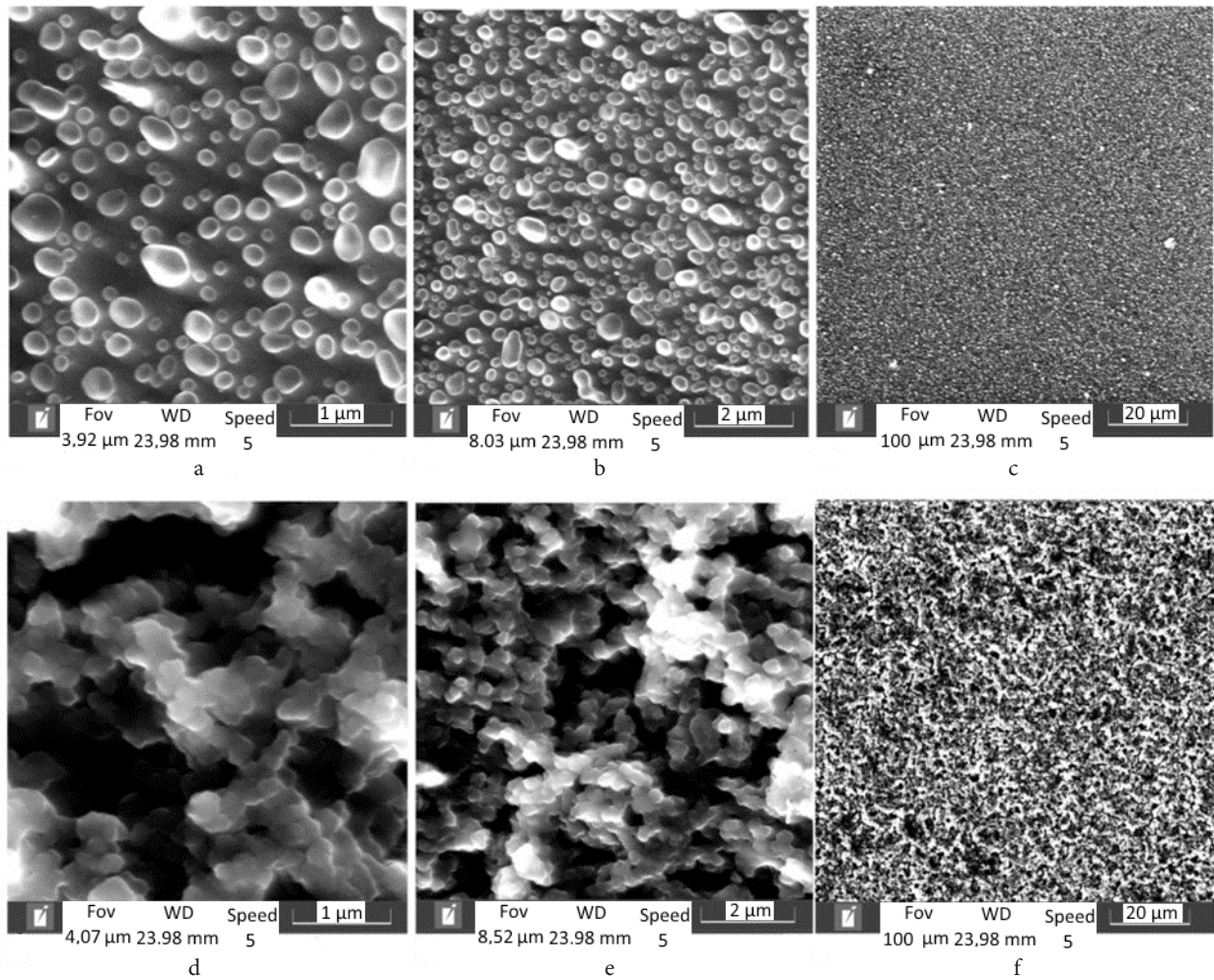


**Fig. 3.** SEM images of microstructures of film samples. The size of the scanning area of the P1 sample (film thickness 500 nm): 4  $\mu\text{m}$  (a), 8  $\mu\text{m}$  (b), 100  $\mu\text{m}$  (c); the P2 sample (film thickness 400 nm): 4  $\mu\text{m}$  (g), 8  $\mu\text{m}$  (d), 100  $\mu\text{m}$  (e).

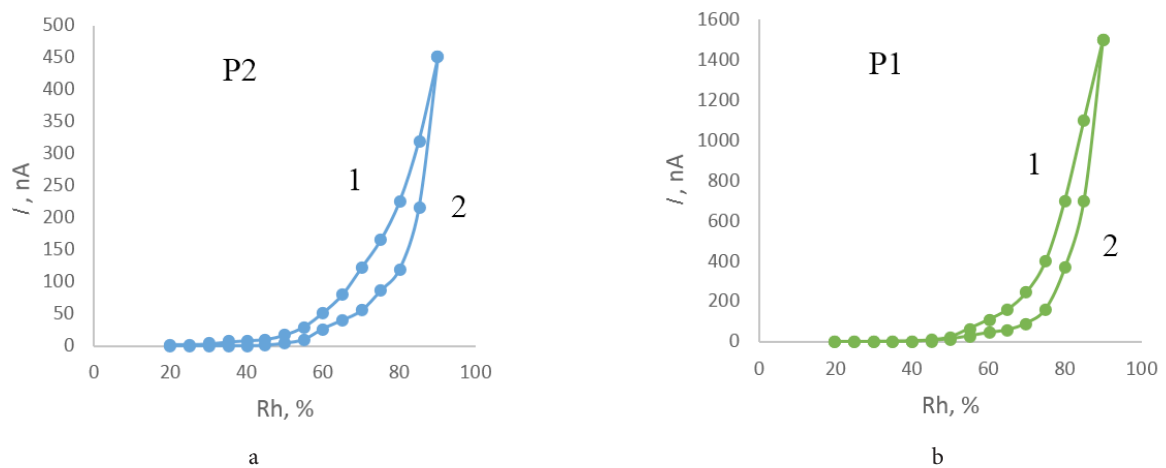


**Fig. 4.** (Color online) Dependence of the current flowing through the P2 and P1 films on the relative humidity of the air in the air volume

**Table 2.** Roughness values of samples.

	P2			P1		
	4 $\mu\text{m}$	8 $\mu\text{m}$	100 $\mu\text{m}$	4 $\mu\text{m}$	8 $\mu\text{m}$	100 $\mu\text{m}$
Root-mean-square roughness in area, nm	225	296	349	230	221	288
Surface area, $\mu\text{m}^2$	144	375	20570	366	695	30950

at the same values of relative humidity (section 1). The higher conductivity of the P1 sample film can be explained by the difference in the polar properties of the substituents in the ortho position and associated with a larger dipole moment of the P1 sample than that of the P2 sample. It is also possible to note a small hysteresis at the P2 sensor (section 2). In the sample of the P2, the hysteresis is by current from 0 to 105 nA, in the P1 from 0 to 400 nA.

For P1, the dipole moment is 1.5421 D, for P2 — 1.5133 D. It can be concluded that P1 has a greater value of the dipole moment, as a result, at the same relative humidity values, the film containing the sample P1 has greater conductivity. When studying the properties of polymers, it is of particular interest to evaluate the polarity of kinetic units — elementary dipoles of monomeric units, since such information helps to study the structure of the corresponding macromolecules. Typically, dipoles in polymers are covalently bound to the main chain of a macromolecule or to its side groups. The dipole moment of a macromolecule, which makes it possible to judge its flexibility, can be defined as the vector sum of the constituent vectors — the dipole moments of the links of chain molecules.

If we assume the articulation of links in a chain molecule to be free and calculate the value of the dipole moment of the monomer, we can judge the flexibility of polymer chains.

The obtained results are explained by the fact that an increase in the electrical conductivity of the polymer film with an increase in ambient humidity is associated with an increase in the mobility of the alloying ion, weakly bound to the polymer chain by Van der Waals forces, or due to the process of protonation of the polymer. When the humidity of the environment increases, the polymer film absorbs moisture, which leads to the swelling of the polymer and the subsequent unfolding of the compact spiral shape of the polymer chain. The formation of a more aligned structure of the PANI derivative facilitates the process of charge transfer along the polymer chain. Adsorption of water molecules on the surface of the polymer film occurs directly due to the formation of a hydrogen bond between water molecules and amino groups in the polymer chain of PANI derivatives. With a further increase in humidity, the formation of several layers consisting of water molecules is possible.

It is also assumed that the saturation of the polymer with moisture can be accompanied by the formation of a complex

due to the transfer of an unshared electron pair from the nitrogen atom of the polymer to the water molecules. Further, after adsorption of moisture on the polymer surface, under the action of an electrostatic field, water molecules can ionize to form hydroxonium ions ( $\text{H}_3\text{O}^+ + \text{H}_2\text{O} \leftrightarrow \text{H}_2\text{O} + \text{H}_3\text{O}^+$ ). The formed hydroxonium ions can participate in the charge transfer process [54]. In addition, it should be noted that at high ambient humidity due to the formation of a network of hydrogen bonds and due to the dissociation of water molecules, proton conductivity of Grothgus can be achieved. Thus, there is a decrease in resistance due to the charge transfer process. It can be assumed that the interaction of the polymer chain with water molecules proceeds similarly to the process of doping the polymer with acid. Nitrogen atoms in amine and imine forms act as acceptor and donor centers, respectively. The imine groups of the polymer chain initiate the process of water dissociation, and the resulting proton is embedded in the  $\pi$ -conjugated polymer chain, which facilitates the electron transfer process. Thus, the possibility of changing the electrical conductivity of PANI derivatives under the influence of the environment is used to create chemical sensors, including humidity sensors, since it is known that the interaction of individual fragments of a polymer molecule with a hydroxyl group or a hydrogen ion can form a charge transfer complex.  $\text{H}^+$  ions in PANI derivatives lead to protonation of the polymer chain; the formation of emeraldine salt and, as a consequence, an increase in electrical conductivity. The properties of synthesized polymers can be improved, but the advantages of polymer organic coatings in the production of electronic materials with unique properties are obvious [55].

The response of the sensors to  $\text{NH}_3$  was estimated from a change in the passing current with a change in the concentration of ammonia vapors.

Films of polyaniline derivatives react to the presence of ammonia vapor in the environment by reducing the flowing current (Fig. 5). The results obtained are explained by the protonation/deprotonation of the polymer chain. An increase in the concentration of ammonia in the medium leads to a decrease in the degree of doping. It is assumed that when the polymer interacts with  $\text{NH}_3$ , ammonia molecules absorb protons from PANI, forming energetically favorable ammonium ( $\text{NH}_4^+$ ), as a result of which PANI deprotonation and conductivity decrease.

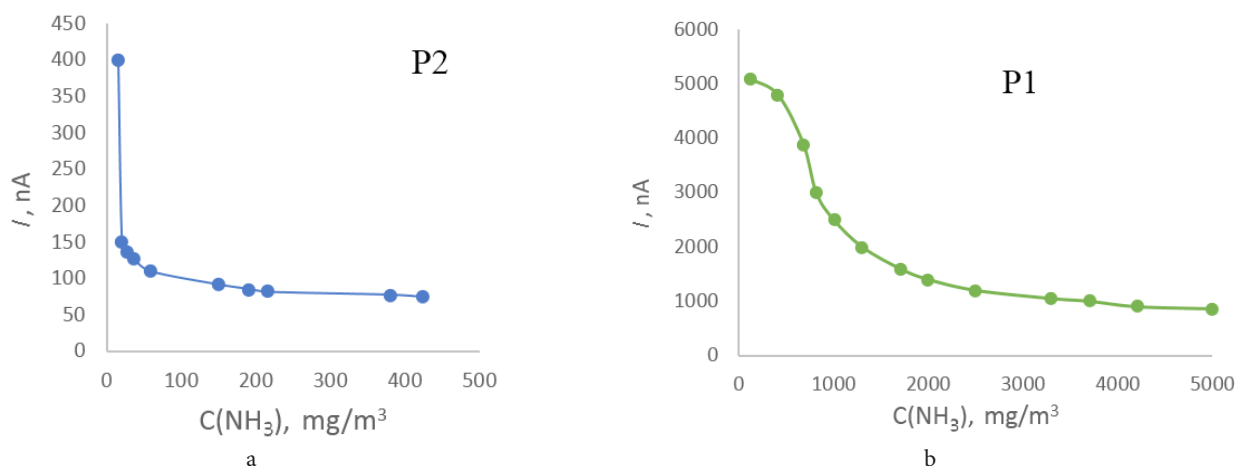


**Fig. 5.** (Color online) Dependences of the current flowing through the P1 and P2 films on the concentration of ammonia vapors, at  $U_{\text{obr}} = 30$  V and room temperature 25°C.

#### 4. Conclusions

The results of the study of the morphology of the surface of the films show the sensitivity is more influenced by the morphology of the surface, its total area, rather than the root mean square roughness, which, taking into account the error, does not differ much from each other for samples P1 and P2.

The sensitivity of P1 films to air humidity is 3 times higher than that of P2 films, which is confirmed by the values of the current flowing through the sample.

P1 films react better to the presence of ammonia vapors in the air, their sensitivity is an order of magnitude higher. It should be noted that thin P2 films show a much greater change in sensitivity to ammonia vapors compared to P1 films, so they possible use of such films in sensors for detecting ultra-low concentrations.

The use of new derivatives of PANI as a detecting element of the sensor allows you to create thin films with a developed surface and well permeable to the analyte. The studied resistive sensors demonstrate very low inertia and good response time. The results showed that the P2 and P1 samples have high sensitivity, fast response time and recovery. Thus, they are of great practical importance in air humidity sensors and sensors for detecting ammonia vapors in.

**Supplementary material.** *The online version of this paper contains supplementary material available free of charge at the journal's Web site (lettersonmaterials.com).*

**Acknowledgements.** *This work was supported by the State assignment for the implementation of scientific research by laboratories (order MN-8/1356 of 09/20/2021).*

#### References

1. B. Adhikari, S. Majumdar. Prog. Polym. Sci. 29, 699 (2004). [Crossref](#)
2. Q. Qi, T. Zhang, Q.J. Yu, R. Wang, Y. Zeng, L. Liu, H.B. Yang. Sens. Actuators B. 133, 638 (2008). [Crossref](#)
3. Q. Qi, T. Zhang, L.J. Wang. Appl. Phys. Lett. 93, 023105 (2008). [Crossref](#)
4. M.V. Arularasu, R. Sundaram, C.M. Magdalane, K. Kanimozhi, K. Kaviyarasu, F.T. Thema, D. Letsholathebe, G.T. Mola, M. Maaza. J Nanostruct. 7, 47 (2017). [Crossref](#)
5. W. Xuan, X. He, J. Chen, W. Wang, X. Wang, Y. Xu, Z. Xu, Y.Q. Fu, J.K. Luo. Nanoscale. 7 (16), 7430 (2015). [Crossref](#)
6. Y. Sakai, Y. Sadaoka, M. Matsuguchi. Sens. Actuators B. 35, 85 (1996). [Crossref](#)
7. Z. Chen, C. Lu. Sens. Lett. 3, 274 (2005). [Crossref](#)
8. Y. Sun, S. Seetharaman, Q. Liu, Z. Zhang, L. Liu, X. Wang. Energy. 114, 165 (2016). [Crossref](#)
9. D. Kassotis, R. Luke, M. Denise, M. Isabelle, C. Adam, H. William, C. Susan. Sci. Total Environ. 557, 901 (2016). [Crossref](#)
10. M. Kaur, B.K. Dadhich, R. Singh, K. Ganapathi, T. Bagwaiya, S. Bhattacharya, A.K. Debnath, K.P. Muthe, S.C. Gadkari. Sens. Actuators B. 242, 389 (2017). [Crossref](#)
11. D. Zhang, J. Wu, Y.Cao. Sens. Actuators B. 287, 346 (2019). [Crossref](#)
12. H. Yang, S. Ma, H. Jiao, Q. Chen, Y. Lu, W. Jin, W. Li, T. Wang, X. Jiang, Z. Qiang, H. Chen. Sens. Actuators B. 245, 493 (2017). [Crossref](#)
13. M. Diana, W. Roekmijati, W. Suyud. EDP Sci. 73, 06003 (2018). [Crossref](#)
14. S. Bardócz. Trends Food Sci. Technol. 6 (10), 341 (1995). [Crossref](#)
15. B. Timmer, W. Olthuis, A. Van Den Berg. Sens. Actuators B Chem. 107, 666 (2005). [Crossref](#)
16. H.Y. Li, C.S. Lee, D.H. Kim, J.H. Lee. ACS Appl. Mater. Interfaces. 10, 27858 (2018). [Crossref](#)
17. H.J. Sharma, D.V. Jamkar, S.B. Kondawar. Proc. Mater. Sci. 10, 186 (2015). [Crossref](#)
18. C. Steffens, M.L. Corazza, E. Franceschi, F. Castilhos, P.S. Herrmann, J.V. Oliveira. Sensors and Actuators B: Chemical. 171–172, 627 (2012). [Crossref](#)
19. H. Xu, D. Ju, W. Li, H. Gong, J. Zhang, J. Wang, B. Cao. Sens. Actuators B. 224, 654 (2016). [Crossref](#)
20. M.T.S. Chani, K.S. Karimov, F.A. Khalid, S.A. Moiz. Solid State Sci. 18, 78 (2013). [Crossref](#)
21. M. Trchová, D. Jasenská, M. Bláha, J. Prokeš, J. Stejskal. Spectrochim Acta A Mol Biomol Spectrosc. 235, 118300 (2020). [Crossref](#)
22. M.V. Kulkarni, A.K. Viswanath. Polym. Eng. Sci. 47, 1621 (2007). [Crossref](#)
23. M.V. Kulkarni, A.K. Viswanath, R.C. Aiyer, P.K. Khanna, J. Polym. Sci. B: Polym. Phys. 43, 2161 (2005). [Crossref](#)
24. M.V. Kulkarni, A.K. Viswanath, P.K. Khanna. Sens. Actuators B Chem. 115, 140 (2006). [Crossref](#)
25. P. Zarrintaj, H. Vahabi, M.R. Saeb, M. Mozafari. In: Fundamentals and Emerging Applications of Polyaniline. Elsevier (2019) p. 259. [Crossref](#)
26. A.N. Andriianova, Yu.N. Biglova, A.G. Mustafin. RSC Adv. 10, 7468 (2020). [Crossref](#)
27. K. Amer, A.M. Elshaer, M.A.S. Ebrahim. J. Mater. Sci. Mater. Electron. 30 (1), 391 (2019). [Crossref](#)
28. G. Liao, Q. Li, Z.Xu. Prog. Org. Coat. 126, 35 (2019). [Crossref](#)
29. G. Čirić-Marjanović. Synth. Met. 177, 1 (2013). [Crossref](#)
30. J. Vivekanandan, V. Ponnusamy, A. Mahudewaran, P. Vijayanand. Arch. Appl. Sci. Res. 3, 147 (2011).
31. J. Liu, X. Hu, X. Wang, J. Yao, D. Sun, Z. Fan, M. Guo. Polym. Int. 63, 722 (2014). [Crossref](#)
32. J. Summers, S. Waware, M. Maduwa, A. Summers. Synth. Met. 209, 251 (2015). [Crossref](#)
33. T. Kabomo, M. Scurrrell. Polym. Adv. Technol. 27, 759 (2016). [Crossref](#)
34. K. Khamngoen, N. Paradee, A. Sirivat. J. Polym. Res. 23, 172 (2016). [Crossref](#)
35. Y. Liu, S. Li, P. Yao, Q. Zhang. Int. J. Mod. Phys. B. 31, 1744091 (2017). [Crossref](#)
36. C. Barbero, H. Salavagione, D. Acevedo, D. Grumelli, F. Garay, G. Planes, M. Miras. Electrochim. Acta. 49, 3671 (2004). [Crossref](#)
37. U.S. Waware. J. Mater. Sci-Mater. El. 28 (20), 15178 (2017). [Crossref](#)
38. U.S. Waware, G.J. Summers, A.M.S. Hamouda, M. Rashid. Polym. Plast. Technol. Eng. 57, 1015 (2018). [Crossref](#)
39. F. Movahedifar, A. Modarresi-Alam. Polym. Adv. Technol. 27 (1), 131 (2016). [Crossref](#)

40. N. R. Tanguy, M. Thompson, N. Yan. *Sens. Actuators B Chem.* 257, 1044 (2018). [Crossref](#)
41. T. Zhang, H. Qi, Z. Liao, Y. D. Horev, L. A. Panes-Ruiz, P. S. Petkov, Z. Zhang, R. Shivhare, P. Zhang, K. Liu, V. Bezugly, S. Liu, Z. Zheng, S. Mannsfeld, T. Heine, G. Cuniberti, H. Haick, E. Zschech, U. Kaiser, R. Dong, X. Feng. *Nat. Commun.* 10, 1 (2019). [Crossref](#)
42. J. Zhao, X. Liu, Y. Wu, D. S. Li, Q. Zhang. *Chem. Rev.* 391, 30 (2019). [Crossref](#)
43. L. R. Latypova, A. N. Andriianova, S. M. Salikhov, I. B. Abdrakhmanov, A. G. Mustafin. *Polymer International.* 69 (9), 804 (2020). [Crossref](#)
44. R. B. Salikhov, Y. N. Biglova, Y. M. Yumaguzin, M. S. Miftakhov, A. G. Mustafin. *Technical Physics Letters.* 39 (10), 854 (2013). [Crossref](#)
45. Z. Du, C. Li, L. Li, H. Yu, Y. Wang, T. Wang. *J. Mater. Sci. Mater. Electron.* 22, 418 (2011). [Crossref](#)
46. A. N. Andrianova. *New polyaniline derivatives: Physico-chemical properties, kinetics and mechanism of formation: PhD thesis.* Bashkir State University, Ufa (2020) 185 p.
47. R. R. Gataullin. *Directed intramolecular cyclization of ORTHO-alkenylanilines: PhD thesis.* UNC RAS, Ufa (2004) 263 p.
48. A. Andriianova, A. Shigapova, Y. Biglova, R. Salikhov, I. Abdrakhmanov, A. Mustafin. *Chinese Journal of Polymer Science.* 37 (8), 774 (2019). [Crossref](#)
49. J. Stejskal, I. Sapurina, M. Trchova, J. Prokes, I. Krivika, E. Tobolkova. *Macromolecules.* 31 (7), 2218 (1998). [Crossref](#)
50. S. Quillard, G. Louarn, J. P. Buisson, M. Boyer, M. Lapkowski, A. Pron. *Synth. Met.* 84, 805 (1997). [Crossref](#)
51. J. G. Masters, Y. Sun, A. G. Macdiarmid, A. J. Epstein. *Synthetic Metals.* 41 (1-2), 715 (1991). [Crossref](#)
52. A. N. Andriianova, T. T. Sadykov, A. Mustafin. *Chemistry Select.* 6 (34), 8942 (2021). [Crossref](#)
53. D. Zhang, D. Wang, P. Li, X. Zhou, X. Zong, G. Dong. *Sens. Actuators, B.* 255 (2), 1869 (2018). [Crossref](#)
54. R. B. Salikhov, A. N. Lachinov, R. G. Rakhmееv, R. M. Gadiev, A. R. Yusupov, S. N. Salazkin. *Measurement Techniques.* 52 (4), 427 (2009). [Crossref](#)
55. A. N. Andriianova, R. B. Salikhov, L. R. Latypova, I. N. Mullagaliev, T. R. Salikhov, A. Mustafin. *Sustainable Energy & Fuels.* 6, 3435 (2022). [Crossref](#)